J. Fluid Mech. (1996), *vol.* 313, *pp.* 283–308

Non-continuum lubrication flows between particles colliding in a gas

By R. R. SUNDARARAJAKUMAR AND DONALD L. KOCH
School of Chemical Engineering, Cornell University, Ithaca, NY 14853, USA

(Received 16 February 1995 and in revised form 1 December 1995)

Solid-body collisions between smooth particles in a gas would not occur if the lubrication force for a continuum incompressible fluid were to hold at all particle separations. When the gap between the particles is of the order of the mean free path λ_0 of the gas, the discrete molecular nature of the gas becomes important. For particles of radii a smaller than about 50 μm colliding in air at a relative velocity comparable to their terminal velocity, the effects of compressibility of the gas in the gap are not important.

The nature of the flow in the gap depends on the relative magnitudes of the minimum gap thickness $h_0 \equiv a\epsilon$, the mean-free path λ_0, and the distance $a\epsilon^{1/2}$ over which the effects of curvature become important. The slip-flow regime, $a\epsilon \gg \lambda_0$, was analysed by Hocking (1973) using the Maxwell slip boundary condition at the particle surface. To find the lubrication force in the transition regime ($a\epsilon \sim O(\lambda_0)$), we use the results of Cercignani & Daneri (1963) for the flux as a function of the pressure gradient in a Poiseuille channel flow. When $a\epsilon \ll \lambda_0 \ll a\epsilon^{1/2}$, one might expect the local flow in the gap to be governed by Knudsen diffusion. However, an attempt to calculate the Knudsen diffusivity between parallel plates leads to a logarithmic divergence, which is cut off by intermolecular collisions, and the flux is therefore proportional to $h_0 \bar{c} \log(\lambda_0/h_0)$, where $\bar{c}$ is the mean molecular speed. The non-continuum lubrication force is shown to have a weak, log-log divergence as the particle separation goes to zero. As a result, the energy dissipated in the collision is finite. In the limit of large particle inertia, the energy dissipated is $6\pi\mu U_0 a^2 (\log h_0/\lambda_0 - 1.28)$, where $2U_0$ is the relative velocity of the particles.

When $\lambda_0 \gg a\epsilon^{1/2}$, we have a free molecular flow in the gap. In this case, owing to the curvature of the particles, the flux versus pressure gradient relation is non-local. We analyse the free molecular flow between two cylinders and obtain scalings for the lubrication force.

1. Introduction

The lubrication forces, which come into play when a fluid is squeezed out of a thin gap between two surfaces, have an important role in many physical applications. Gas–solid flows such as those occurring in pneumatic transport and fluidized beds are influenced by the fluid dynamic forces in the gas as well as forces associated with solid-body contacts between the particles. In cloud physics applications, the rate of raindrop coalescence is of interest (see Ochs & Beard 1985) and this rate is influenced by a variety of factors such as the gas dynamic forces, particle inertia, and electrostatic and van der Waals forces. The efficiency of particulate removal methods, such as cyclone

separation, electrostatic precipitation and filtration, is greatly influenced by the rate of coagulation. In all these cases, a detailed microscale study of the lubrication flow is essential to an accurate description of the physical process involved. Any such detailed study must address the question of why the continuum lubrication forces, which grow like $1/h$ with decreasing particle separation h, do not prevent solid-body collisions.

The absence of such an analysis has resulted in a variety of approximations. Early descriptions of raindrop coalescence (Hocking & Jonas 1970) used a cutoff distance below which the particles were considered to undergo a collision. This led to an underprediction of the rate of coalescence. Models of cyclones which neglect particle–particle coalescence underpredict the collection efficiency in the 0.5–20 μm diameter range (Bohnet 1983).

In theories of rapid granular flow (Jenkins & Savage 1983), the particles are assumed to undergo solid-body collisions. The loss of energy during these collisions is given in terms of a lumped parameter – the coefficient of restitution, e, which is the ratio of the relative velocity along the line-of-centres of the particles after and before collision. The loss of energy during the collision is typically associated with the inelasticity of the particles. However, for sufficiently small particles or for particles colliding with sufficiently small relative velocities, the dissipation resulting from the lubrication flow in the gas between the particles may become comparable to the loss of energy due to the inelasticity of the solid. For particle diameters less than about 100 μm, a significant part of the energy dissipation is due to viscous forces; for larger particles and sufficiently large impact velocities, effects of solid-body inelasticity dominate.

In theories of dilute gas–solid suspensions (Koch 1990; Kumaran & Koch 1993), the dissipation due to lubrication interactions has been neglected compared to the viscous dissipation caused by the drag force between particle collisions. However, in a dense fluidized bed, the particle separations are always small compared to the particle radius and the lubrication losses can no longer be neglected. Moreover, it is important to know the rate of energy dissipation in order to determine the stability criterion for the fluidized bed.

1.1. *Mechanisms of lubrication breakdown*

For particle separations comparable with the mean free path of the gas, the equations of continuum fluid mechanics no longer hold. It is reasonable to expect that the breakdown of the continuum will lead to a decrease in the lubrication force. Hocking included the first effects of discrete molecular flow in a calculation of the lubrication force on a spherical particle, by using the Maxwell slip boundary condition. However, the Maxwell slip model is valid only in the limit $h_0 \gg \lambda_0$. Hence, Hocking's analysis alone cannot give quantitative results for the lubrication force at separations comparable with λ_0. Under atmospheric conditions, the mean free path λ_0 is about 0.1 μm. In this paper, we present detailed calculations of the lubrication flow for gap thicknesses comparable to and much less than the mean free path.

Another factor which may modify the lubrication force at small particle separations is the roughness of the particle surface. While particle roughness is important in many practical situations, one may study particles that are smooth on length scales comparable to the mean free path. Such a study has the advantage that the lubrication flow will not be affected by properties of the particle surface that are difficult to measure or control. Even in cases where particle roughness plays a significant role, one may ask what causes the breakdown of lubrication flow between the asperities.

The physical mechanisms modifying lubrication flows between particles colliding in a liquid are different from those in a gas. Davis *et al.* (1986) have studied the

elastohydrodynamic collisions between particles suspended in a liquid. Throughout these collisions, the particles are separated by a viscous liquid film. The pressure forces in this lubrication film are sufficiently large to cause the particles to deform and rebound without making solid-body contact. Because of the relatively low dynamic viscosity of a gas, the pressure in the lubricating gas considered here will not be sufficient to cause significant deformation. Davis *et al.* used the dimensionless elasticity parameter $\eta = 8(1-\nu^2)\mu U_0 a^{3/2}/\pi E h_0^2$ to quantify the tendency of the solids to deform. Here, ν is the Poisson's ratio, E the Young's modulus, and μ the viscosity of the fluid. $2U_0$ is the initial relative velocity of the particles, a the particle radius, and h_0 the separation between the particles. In order to neglect the particle deformation when $h = h_0$, the parameter η must be small compared to unity. For 50 μm radius sandstone particles colliding in air at a relative velocity equal to their terminal velocity, we can estimate this parameter at a separation $h_0 = \lambda_0$. With particle density $\rho_s = 2.2\ \mathrm{g\,cm^{-3}}$, $\mu = 0.017$ cP, $\nu \approx 0.1$, $E = 5.7 \times 10^{11}\ \mathrm{dyn\,cm^{-2}}$, $U_0 = 35\ \mathrm{cm\,s^{-1}}$, and $h_0 = 0.1\ \mu\mathrm{m}$, the parameter η is as small as 1×10^{-7}. Note that for 50 μm radius particles colliding in air, lubrication forces come into play when the separation is around 5 μm. Consequently, the use of the terminal velocity at a separation of the order of mean free path provides an overestimate of the deformation.

For sufficiently small particles and low velocities, van der Waals attractions may lead to particle contact. However, an estimate of the van der Waals force for silica glass spheres of 25 μm radius colliding with a relative velocity comparable to their terminal velocity indicates that it is a small fraction (on the order of 10^{-3}) of the lubrication force for separations comparable to the mean free path. It may also be noted that van der Waals forces are conservative and so cannot modify the singular energy dissipation associated with the application of continuum lubrication to all particle separations.

A salient feature of lubrication flows is the large pressure drop that is required to drive the fluid out of a thin gap. If this pressure change becomes comparable to the atmospheric pressure, then the integral mass balance must be modified to account for the effects of the compressibility of the gas. The pressure drop in the gap scales like $\mu U a/h_0^2$. Thus, it is clear that the effects of compressibility of the gas can be neglected for $h_0 \gg h_c = (\mu U a/p_0)^{1/2}$.

The relative importance of compressibility and discrete molecular effects may be expressed in terms of the dimensionless parameter $\alpha = h_c/\lambda_0$, which increases with increasing particle radius and relative velocity. For 50 μm radius particles colliding with a relative velocity comparable to their terminal velocity, h_c is comparable to the mean-free path and the effects of compressibility and discrete molecular flow are equally important. The effects of compressibility on the collision of particles in liquids has been analysed by Barnocky & Davis (1989) and by Kytömaa & Schmid (1992) and we plan to consider compressible gas lubrication flows between colliding particles in a future publication.

In this paper we analyse the case of incompressible discrete molecular flows, which correspond to the limit $\alpha \ll 1$. In §2 we analyse the lubrication flow between two spheres. In §3 we study the lubrication flow between two cylinders. Specifically, in §2.1 we show that the lubrication force for two spheres has a weak, log-log divergence as the particle separation goes to zero. In §2.2, we calculate the energy loss in the collision of two spheres. In the limit of large particle inertia, i.e. high Stokes number, the energy lost in the collision is shown to be $6\pi\mu a^2(\log h_0/\lambda_0 - 1.28)$. Numerical results for the energy loss as a function of Stokes number for different

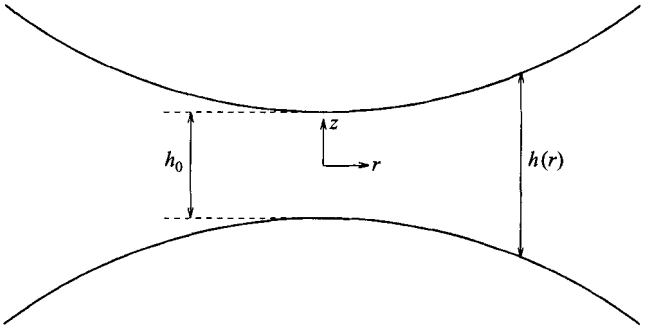

FIGURE 1. Schematic showing two spheres of radius a approaching each other along their line-of-centres. Here, r is the radial coordinate in the plane normal to the line-of-centres. The gap thickness is $h(r) = h_0 + r^2/a$, where h_0 is the minimum separation between the particle surfaces.

initial separations of the colliding particles are also presented. In § 3.1, we study the lubrication flow between two cylinders when $\lambda_0 \ll a\epsilon^{1/2}$. In § 3.2, we study the free molecular flow ($\lambda_0 \gg a\epsilon^{1/2}$) between two cylinders. Finally, in § 4, we summarize the results of this study, and based on physical arguments, we present scalings for the lubrication force for colliding spheres in the free molecular flow limit.

2. Collision of spheres

2.1. *Pressure profiles and force for* $\lambda_0 \ll a\epsilon^{1/2}$

In the usual analysis for incompressible continuum lubrication flow between two particles, the flow is approximated locally as a pressure driven unidirectional flow between two flat plates separated by a distance that changes with radial position according to $h(r) = h_0 + r^2/a$ (see figure 1). Here, h_0 is the minimum gap thickness, r the radial distance from the line-of-centres of the particles and a the reduced radius defined by $a = 2a_1a_2/(a_1 + a_2)$, where a_1 and a_2 are the radii of the two colliding particles. (Note that with this definition of a, our results are applicable to collisions between unequal-sized spheres as well as particle–wall collisions.) The radial flux of the fluid is determined from an integral mass balance. Then the pressure drop required to achieve this radial flux is obtained assuming a local Poiseuille channel flow in the gap. The lubrication force is then found by integrating the pressure over the particle surface. In the case of spheres, this leads to a force that is inversely proportional to the gap thickness. If this force were applied at all separations, the kinetic energy of the particles would be completely dissipated by viscous forces and the particles would not touch in a finite time. Clearly, the familiar incompressible continuum lubrication analysis is inadequate.

Hocking (1973) modified the standard lubrication analysis to include the first effects of the discrete nature of the molecular gas in the limit $\delta_0 \gg 1$, where $\delta_0 \equiv a\epsilon/\lambda_0$ is the inverse Knudsen number based on the minimum gap thickness $a\epsilon \equiv h_0$. This was done by using the Maxwell slip boundary condition instead of the usual no-slip condition at the particle surfaces. The slip-flow approximation sets the relative velocity at the boundary to be proportional to the gradient of the tangential velocity – the constant of proportionality being of the order of the mean-free path. That is

$$u_r \mp \frac{k_1}{\delta_0} \frac{\partial u_r}{\partial z} = 0 \text{ on } z = \pm h/2,$$

where $k_1\lambda_0$ is the slip coefficient. For a hard-sphere gas, $k_1 = 1.1081$ (Loyalka & Ferziger 1967). (It may be noted that the value of the slip coefficient for molecules interacting via a non-hard-core potential is close to the corresponding hard-sphere value.) Hocking's analysis gives the following expression for the pressure as a function of radial distance:

$$p(r) - p_0 = \frac{-\delta^2}{2(3k_1)^2}\left(\log(1+\frac{6k_1}{\delta}) - \frac{6k_1}{\delta}\right), \tag{2.1}$$

where the pressure has been non-dimensionalized with $3\mu Ua/h^2$, the lubrication pressure in the continuum case. Distances in the r- and z-directions are scaled with $a\epsilon^{1/2}$ and $a\epsilon$ respectively, and $\delta(r) = \delta_0(1+r^2)$. The force acting on each sphere is given by

$$f = \frac{\delta_0}{2(3k_1)^2}\left((\delta_0 + 6k_1)\log(1+6k_1/\delta_0) - 6k_1\right), \tag{2.2}$$

where the force is scaled with the continuum lubrication resistance $3\pi\mu Ua^2/h_0$. The dimensional force given by the above equation diverges only logarithmically as the gap thickness goes to zero. This leads to a prediction of particle contact in a finite time. However, Hocking's analysis is valid only for $\delta_0 \gg 1$. For sufficiently small gap thicknesses, δ_0 can become an order-one quantity or even smaller. Thus, Hocking's analysis alone is not enough to describe the flow in the gap for all particle separations.

When the gap thickness is comparable to the mean free path ($\delta \equiv h/\lambda_0 \sim 1$), the flow in the gap is governed by the Boltzmann equation:

$$\frac{\partial}{\partial\tilde{t}}(n\tilde{f}) + \tilde{c}_r\frac{\partial}{\partial\tilde{r}}(n\tilde{f}) + \tilde{c}_z\frac{\partial}{\partial\tilde{z}}(n\tilde{f}) = J(n\tilde{f}, n\tilde{f}), \tag{2.3}$$

where $n(\boldsymbol{x})$ is the number density, $\tilde{f}$ is the velocity distribution function and J is the nonlinear collision integral. Scaling $\tilde{t}$ with $(a\epsilon/U)$, $\tilde{r}$ with $a\epsilon^{1/2}$, $\tilde{z}$ with $a\epsilon$, and $\tilde{\boldsymbol{c}}$ with the mean molecular speed $\bar{c}$, it can be seen that the time-derivative term is $O(U/\bar{c})$. For incompressible flows, $U/\bar{c} \ll 1$, and hence the time-derivative term can be dropped. We now observe that the z-component of the average gas velocity $\tilde{u}_z$ is $O(U)$. To estimate the size of the radial component $\tilde{u}_r$ of the average gas velocity, we turn to the mass conservation equation, which can be derived by averaging the Boltzmann equation over the velocity space:

$$\frac{1}{\tilde{r}}\frac{\partial}{\partial\tilde{r}}(\tilde{r}\tilde{u}_r) + \frac{\partial}{\partial\tilde{z}}(\tilde{u}_z) = 0, \tag{2.4}$$

where we have assumed the gas to be incompressible. Using the scalings already mentioned for $\tilde{z}$, $\tilde{x}$, and $\tilde{u}_z$, we conclude that $\tilde{u}_r \sim U\epsilon^{-1/2}$. The scalings up to this point are similar to the familiar scalings in the continuum lubrication problem. However, when we have significant rarefaction ($\delta \sim 1$), we cannot use the continuum Navier–Stokes equations. Instead, we must solve for the velocity distribution function, from which all macroscopic quantities of interest can be calculated. In general, the nonlinear Boltzmann equation (2.3) is difficult to solve.

For nearly incompressible flows ($U/\bar{c} \ll 1$), we can linearize $\tilde{f}$ by writing $\tilde{f} = \tilde{f}_0(1+\tilde{\phi})$, ($|\tilde{\phi}| \ll 1$), where

$$\tilde{f}_0 = \left(\frac{m}{2\pi kT}\right)^{3/2}\exp\left(\frac{-m\tilde{c}^2}{2kT}\right).$$

In order to estimate the size of $\tilde{\phi}$, we observe that, by mass conservation, the

macroscopic gas velocity in the radial direction is $O(\epsilon^{-1/2})$ larger than that in the z-direction. In other words

$$\left| \int \tilde{f}_0(1+\tilde{\phi})\boldsymbol{c}\mathrm{d}\boldsymbol{c} \right| = |\boldsymbol{u}| \sim U\epsilon^{-1/2},$$

from which it is clear that $\tilde{\phi} \sim U/\bar{c}\epsilon^{1/2}$. Thus, the Boltzmann equation can be linearized if $U/\bar{c} \ll \epsilon^{1/2}$.

Before we write the linearized Boltzmann equation, it will be useful to obtain scaling estimates for the variation of number density in the r- and z-directions. For this we use the following momentum conservation equation:

$$\frac{\partial \rho \tilde{\boldsymbol{u}}}{\partial \tilde{t}} + \nabla \cdot (\rho \tilde{\boldsymbol{u}}\tilde{\boldsymbol{u}}) = \nabla \cdot \tilde{\sigma}, \tag{2.5}$$

where ρ is the mass density and $\tilde{\sigma} = -\int \tilde{f}\,\tilde{\boldsymbol{c}}\tilde{\boldsymbol{c}}\,\mathrm{d}\tilde{\boldsymbol{c}}$ is the stress tensor. We now non-dimensionalize $\tilde{\sigma}$ with $\rho\bar{c}^2$ and use cylindrical coordinates (r, θ, z). It can be seen from the scaled r-component of the momentum equation that the inertial terms are $O(U^2\epsilon^{-1/2}/\bar{c}^2)$. Using $\tilde{\phi} \sim U\epsilon^{-1/2}/\bar{c} \ll 1$, we can neglect the inertial terms from the r-momentum equation. By a similar argument, the inertial terms in the z-momentum equation can also be neglected. Now, using $\tilde{f} = \tilde{f}_0(1+\tilde{\phi})$, $\tilde{\phi} = U\epsilon^{-1/2}\phi/\bar{c}$, the r-momentum equation can be written as

$$\frac{\epsilon\bar{c}}{U}\frac{1}{n}\frac{\partial n}{\partial r}\int f_0 c_r c_r \mathrm{d}\boldsymbol{c} + \epsilon^{1/2}\int f_0\left(\frac{c_r c_r}{r}\frac{\partial}{\partial r}r\phi - \phi c_\theta c_\theta\right)\mathrm{d}\boldsymbol{c} + \int f_0 \frac{\partial \phi}{\partial z} c_r c_z \mathrm{d}\boldsymbol{c} = 0.$$

From this, we conclude that the radial variations in the number density are $O(nU/\bar{c}\epsilon)$. Similarly, the z-momentum equation can be written as

$$\left(\frac{\epsilon\bar{c}}{U}\right)\frac{1}{n}\frac{\partial n}{\partial z}\int f_0 c_z c_z \mathrm{d}\boldsymbol{c} + \epsilon^{1/2}\left(\int f_0 \frac{\partial \phi}{\partial r} c_r c_z \mathrm{d}\boldsymbol{c} + \int f_0 \frac{\partial \phi}{\partial z} c_z c_z \mathrm{d}\boldsymbol{c}\right) = 0.$$

Hence we conclude that the $O(nU/\bar{c}\epsilon^{1/2})$ number density variations in the z-direction can be neglected, compared to the $O(nU/\bar{c}\epsilon)$ variations in the r-direction.

The linearized Boltzmann equation takes the form

$$\epsilon^{1/2} c_r \frac{\partial \tilde{\phi}}{\partial r} + \epsilon^{1/2}\frac{1}{n}\frac{\mathrm{d}n}{\mathrm{d}r}c_r + c_z\frac{\partial \tilde{\phi}}{\partial z} = \left(\frac{a\epsilon}{\bar{c}}\right)\tilde{L}\tilde{\phi}, \tag{2.6}$$

where $\tilde{L}$ is the linearized collision operator. Assuming diffuse reflection, the following linearized boundary condition holds at the surface of each particle:

$$\tilde{f} = \tilde{f}_0\left(1 + \frac{m}{kT}\tilde{\boldsymbol{c}} \cdot \boldsymbol{U}\right) \quad \text{on } \partial S,\ \tilde{\boldsymbol{c}} \cdot \boldsymbol{n} > 0,$$

where $\boldsymbol{U}$ is the velocity of the particle, ∂S denotes the particle surface, and $\mathbf{n}$ is the unit outward normal to the surface. In terms of $\tilde{\phi}$, this can be written as

$$\tilde{\phi} = \frac{m}{kT}\tilde{\boldsymbol{c}} \cdot \boldsymbol{U} \quad \text{on } \partial S,\ \tilde{\boldsymbol{c}} \cdot \boldsymbol{n} > 0.$$

Using the scaling for $\tilde{\phi}$, this can be written as

$$\phi = \mp\epsilon^{1/2}\frac{\pi}{8}\boldsymbol{c} \cdot \boldsymbol{e}_z \quad \text{on } \partial S, \boldsymbol{c} \cdot \boldsymbol{n} > 0,$$

where we have written $\boldsymbol{U} = \mp U\boldsymbol{e}_z$ for the velocity of the top and bottom spheres respectively. Hence we conclude that, to leading order, ϕ is zero on the particle

surfaces. This is equivalent to saying that, to leading order, the molecules emitted from the surface have a distribution $\tilde{f}_0$. We now observe that $\tilde{L}\tilde{\phi}$ scales like $\tilde{\phi}\bar{c}/\lambda_0$, and rewrite (2.6) accordingly:

$$\left.\begin{aligned} \frac{\bar{c}\epsilon}{U}\frac{1}{n}\frac{\mathrm{d}n}{\mathrm{d}r}c_r + c_z\frac{\partial\phi}{\partial z} &= \frac{a\epsilon}{\lambda_0}L\phi, \\ \phi = 0 \ \text{ on } \partial S, \ \boldsymbol{c}\cdot\boldsymbol{n} &> 0, \end{aligned}\right\} \tag{2.7}$$

where we have dropped the radial derivative of ϕ, which is $O(\epsilon^{1/2})$ smaller than the other terms. Equation (2.7) represents the pressure-driven flow of a rarefied gas in a channel. Hence, the flow in the gap can be approximated locally as a Poiseuille flow between two flat plates – as is done for the continuum lubrication problem.

Hickey & Loyalka (1990) have solved the linearized Boltzmann equation for the pressure-driven flow between two flat plates. In addition to this exact calculation, there are calculations which solve an approximate form of the Boltzmann equation (for example, Cercignani & Daneri 1963). The results of Cercignani & Daneri are in good agreement with the solution of Hickey & Loyalka. We shall use the results of Cercignani & Daneri, because their calculations provide results for the flux due to a given pressure gradient over a wider range of inverse Knudsen numbers δ. These results for the transition regime ($\delta \sim 1$) flux, along with the flux corresponding to the limit of small δ, derived in the Appendix, will then be used to obtain the pressure profiles and to compute the force acting on the particles.

For very small gap thicknesses $h_0 \ll \lambda_0$, one might expect the flow in the gap to be governed by a Knudsen diffusion of the gas molecules between the particles (approximated locally as two flat plates). However, an attempt to calculate the Knudsen diffusivity for pressure-driven flow between two flat plates leads to a logarithmically divergent integral. This divergence is due to molecules which travel large distances nearly parallel to the walls. The divergence may be removed by the inclusion of one of two physical effects: (i) A molecule that travels a distance of the order of λ_0 undergoes an intermolecular collision and is likely to be driven to the wall in a short, $O(a\epsilon)$ distance. A derivation of this 'pseudo-Knudsen' flux is given in the appendix. (ii) If the molecule travels a distance comparable to $a\epsilon^{1/2}$, the curvature of the particles will become important and the molecule's flight cannot be approximated as a flight between two flat plates of infinite extent. The spatial variations in the pressure gradient also become important in this case.

Either of the two physical effects described above can be important depending on the relative size of the mean free path λ_0 and the length scale $a\epsilon^{1/2}$ on which curvature becomes important. When $\lambda_0 \gg a\epsilon^{1/2}$, we have a free molecular flow in the gap. In this case, we have

$$\tilde{\boldsymbol{c}}\cdot\frac{\partial\tilde{f}}{\partial\tilde{\boldsymbol{x}}} = 0. \tag{2.8}$$

In § 3, we illustrate the nature of free molecular flow ($\lambda_0 \gg a\epsilon^{1/2}$) by studying the collision of cylinders.

The computation of the lubrication force proceeds as follows. For small δ, we use the pseudo-Knudsen flux derived in the Appendix, along with the transition-regime ($\delta \sim 1$) numerical data for flux from Cercignani & Daneri (1963), to obtain the pressure profiles. We then combine these with the expression for pressure given by Hocking (1973), which is valid for $a\epsilon \gg \lambda_0$, to obtain the pressure as a function of the

radial distance for all gap thicknesses. Using this pressure profile, we obtain the force acting on the particles as a function of minimum gap thickness.

The expression relating the flux to the pressure gradient is obtained from the following integral mass balance equation:

$$\frac{1}{r}\frac{\mathrm{d}}{\mathrm{d}r}\left(r\int_{-\bar{h}/2}^{+\bar{h}/2} u_r\,\mathrm{d}z\right) = 2, \tag{2.9}$$

where $\bar{h}(r) = 1+r^2$ is the scaled gap thickness. If n_0 is the equilibrium number density, then the flux, $q(r)$, scaled with $n_0\bar{c}\epsilon^{-1/2}$ is given by $q(r) = (U/\bar{c})(1/\bar{h})\int_{-\bar{h}/2}^{+\bar{h}/2} u_r\,\mathrm{d}z$. Making use of the fact that the flux is finite at $r = 0$, $\delta = h/\lambda_0$, and integrating (2.9), we obtain

$$q(r) = \left(\frac{U}{\bar{c}}\right)\frac{\delta_0 r}{\delta(r)}. \tag{2.10}$$

If the pressure profile is linear on the length scale of the mean free path, the flux is a function of the local pressure gradient. This will be true as long as $\lambda_0 \ll a\epsilon^{1/2}$. Hence the flux can be written as

$$q(\delta) = -\left(\frac{\lambda_0}{ap_0}\right)\delta\, g(\delta)\frac{\mathrm{d}p}{\mathrm{d}r}, \tag{2.11}$$

where $g(\delta)$ is a dimensionless factor which depends on the geometry of the flow region and on the relative size of the mean free path and the gap thickness. The function $g(\delta)$ is given by

$$g(\delta) = \begin{cases} \frac{1}{4}\,(-\log\delta + 0.4513) & (\delta \ll 1) \\ V(\delta) & (\delta_1 < \delta < \delta_2) \\ \dfrac{\pi}{48}\,\delta + 0.4502 & (\delta \gg 1)\ , \end{cases} \tag{2.12}$$

where the function $V(\delta)$ has been tabulated by Cercignani & Daneri (1963)†. The expressions for g in the limits $\delta \ll 1$ and $\delta \gg 1$ are asymptotic and this makes Cercignani & Daneri's computed values of g at the cutoff points (δ_1, δ_2) slightly different from those given by the corresponding asymptotic expressions. Hence we have used a curve fit to effect smooth transitions across the different regimes. The solid line in figure 2 is the smooth curve for g used in our calculations. The dotted curves are the asymptotic expressions for g in the pseudo-Knudsen and slip-flow regimes. In the transition regime, the difference between the computed values of Cercignani & Daneri and our fitted curve is so small as to make them indistinguishable in this plot.

Using (2.9) and (2.10), and scaling p with the continuum lubrication pressure $3\mu Ua/h^2$, we obtain

$$\frac{\mathrm{d}(p/\delta^2)}{\mathrm{d}r} = \left(\frac{\pi}{24}\right)\frac{1}{\delta^2\, g(\delta)}. \tag{2.13}$$

The pressure profiles plotted in figure 3 are computed using the curve fit for $g(\delta)$ and integrating the above expression numerically. However, to facilitate subsequent asymptotic analysis of the force resisting motion, we also use the expression (2.12) for $g(\delta)$ to obtain analytical expressions for the pressure in the various regimes. For

† In the notation of Cercignani & Daneri, the function $(\pi/4^{1/2})\,V(\pi\delta/2^{1/2})$ is denoted by $Q(\delta)$.

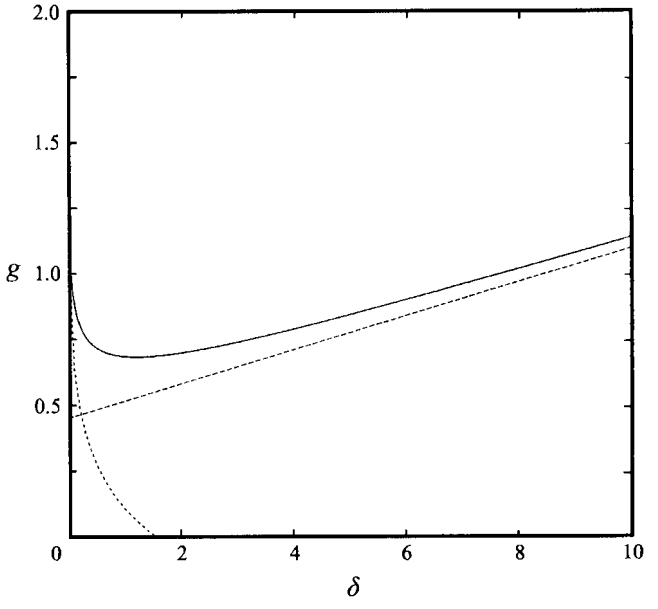

FIGURE 2. The function $g(\delta)$ appearing in the expression for flux. The solid line is the smooth curve used in our calculations and the two dotted curves are the asymptotic expressions in the two limits $\delta \ll 1$ and $\delta \gg 1$.

this purpose, we choose $\delta_1 = 0.1$ as the cutoff for pseudo-Knudsen flux and $\delta_2 = 10$ as the cutoff for the transition regime flux, and thus obtain

$$p(r) - p_0 = \begin{cases} \delta^2 \left[p_1 + p_2 + \dfrac{\pi}{6} e^b \displaystyle\int_{\theta_1}^{\theta(r)} \frac{e^s}{s}\, ds \right] & (\delta \leqslant \delta_1) \\ \delta^2 \left[p_2 - \dfrac{\pi}{24} \displaystyle\int_{\delta_2}^{\delta(r)} \frac{dt}{t^2 g(t)} \right] & (\delta_1 \leqslant \delta \leqslant \delta_2) \\ \dfrac{-\delta^2}{2(3k_1)^2} \left[\log\left(1 + \dfrac{6k_1}{\delta}\right) - \dfrac{6k_1}{\delta} \right] & (\delta > \delta_2)\,, \end{cases} \tag{2.14}$$

where $\delta = \delta_0(1 + r^2)$, $\theta = \log(1/\delta) - b$, and $b = -0.4513$. The quantities p_1 and p_2 are related to the pressure drops over the transition and slip-flow regimes respectively. The expressions for p_1 and p_2 are

$$p_1 = \frac{\pi}{24} \int_{\delta_1}^{\delta_2} \frac{dt}{t^2 g(t)}\,,$$

$$p_2 = \frac{-1}{2(3k_1)^2} \left(\log\left(1 + \frac{6k_1}{\delta_2}\right) - \frac{6k_1}{\delta_2} \right),$$

where r_1 and r_2 are the radial distances at which the inverse Knudsen number δ attains the values 0.1 and 10.0 respectively. That is, r_i $(i = 1, 2)$ are defined for $\delta_i > \delta_0$ by $r_i = (\delta_i/\delta_0 - 1)^{1/2}$.

The pressure profiles are plotted in figure 3. The abscissa is the non-dimensional radial distance. The ordinate is the pressure non-dimensionalized by the continuum lubrication pressure at the same radial position. The different curves are for different

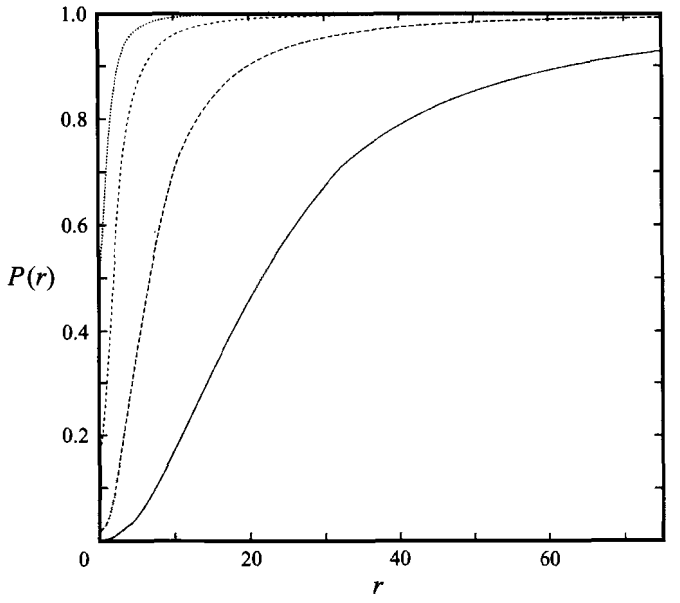

FIGURE 3. The pressure in the gap as a function of the radial distance for various non-dimensional minimum gap thicknesses: ——, $\delta_0 = 0.01$; – – –, $\delta_0 = 0.1$; – – – –, $\delta_0 = 1.0$; ·····, $\delta_0 = 5.0$. The pressure is scaled with $3\mu Ua/h^2$, where $h(r)$ is the gap thickness. The radial distance is scaled with $ae^{1/2}$.

inverse Knudsen numbers δ_0, based on the minimum gap thickness. As one would expect, the pressure approaches the continuum value as the gap thickness increases.

The force resisting the relative motion of the two particles is found by integrating the numerically obtained pressure profiles across the particle surface. Before discussing the results of our computation, it is of interest to obtain an analytical expression for the force, using (2.14). For this, we non-dimensionalize the force with $3\pi\mu Ua^2/h_0$, which is the incompressible continuum lubrication resistance for the normal motion of two spheres. The non-dimensional expression for the force is

$$f = \begin{cases} \dfrac{\pi}{6}\left[\delta_0 \log\left(\dfrac{\log(1/\delta_0)-b}{\log(1/\delta_1)-b}\right) - \delta_0^2\, \mathrm{e}^b \displaystyle\int_{\theta_1}^{\theta_0} \frac{\mathrm{e}^s}{s}\,\mathrm{d}s\right] + \frac{\pi}{24}\delta_0 \int_{\delta_1}^{\delta_2} \frac{\mathrm{d}t}{t\,g(t)} \\ \qquad +\delta_2\delta_0\, p_2 - \delta_0^2\,(p_1+p_2) + k_2\,\delta_0 \qquad (\delta_0 \ll 1) \\ \dfrac{\pi}{24}\,\delta_0 \displaystyle\int_{\delta_0}^{\delta_2} \frac{(t-\delta_0)}{t^2\,g(t)}\,\mathrm{d}t + \delta_0\,(\delta_2-\delta_0)p_2 + k_2\,\delta_0 \qquad (\delta_1 \leqslant \delta_0 \leqslant \delta_2) \\ \dfrac{\delta_0}{2(3k_1)^2}\left[(6k_1+\delta_0)\log(1+6k_1/\delta_0) - 6k_1\right] \qquad (\delta_0 \gg 1), \end{cases} \tag{2.15}$$

where

$$k_2 = \frac{1}{2(3k_1)^2}\left[(6k_1+\delta_2)\,\log(1+6k_1/\delta_2) - 6k_1\right].$$

We note that the force on the particle diverges like $\log\log(1/\delta_0)$ in the limit $a\epsilon \ll \lambda_0 \ll a\epsilon^{1/2}$. The energy dissipated, is thus controlled by the case $a\epsilon \geqslant O(\lambda_0)$.

In figure 4(*a*), the non-continuum lubrication resistance (2.15) is plotted as a function of inverse Knudsen number δ_0. The force is non-dimensionalized with $3\pi\mu U a^2/h_0$, so that the ordinate 1 on the plot corresponds to the incompressible continuum lubrication resistance. It can be seen that, as required, the non-continuum lubrication force approaches the continuum lubrication force for large gap thicknesses. From this plot it can also be seen that the force due to a non-continuum flow is less than that due to a continuum flow. However, the non-continuum force given by equation (2.15) is still divergent as $\delta \to 0$. This divergent behaviour is not apparent in this plot because of the particular non-dimensionalization for force that we have chosen.

In figure 4(*b*), the lubrication resistance scaled with $3\pi\mu U a^2/\lambda_0$ is plotted as a function of δ_0. The lower curve (solid line) is the lubrication resistance for the incompressible non-continuum case. The dotted curve is the usual continuum incompressible lubrication resistance. The continuum lubrication force diverges as $1/\delta_0$, while the non-continuum lubrication resistance diverges only like $\log\log(1/\delta_0)$. The weaker divergence can be observed in this plot.

Our results for the force, together with those of Ying & Peters (1989), who solved for the relative mobility of two spheres for small but finite values of the Knudsen number $Kn = \lambda_0/a$, can be used to obtain the relative mobility over the full range of separations. It may be noted that while the results of Ying & Peters are applicable for $h_0 \gg \lambda_0$ with no restriction on h_0/a, our results hold for $h_0 \ll a$ with no restriction on h_0/λ_0.

In principle, (2.15) can be used to compute the force for any particle separation. However, it is quite cumbersome and is in a form that entails considerable computational cost – especially so for dynamic simulations of hydrodynamically interacting particles. We give below a simple fit for the actual force expression, accurate to within 2% of the actual force and continuous for all values of δ_0:

$$f_{fit} = \begin{cases} \dfrac{\pi}{6}\left(\log t - \dfrac{1}{t} - \dfrac{1}{t^2} - \dfrac{2}{t^3}\right) \\ \qquad +2.587\,\delta_0^{\,2} + 1.419\,\delta_0 + 0.3847 \\ \qquad -1.378\times 10^{-3}\,\delta_0^{\,5} + 2.199\times 10^{-2}\,\delta_0^{\,4} \qquad (\delta_0 < 0.26) \\ -0.1359\,\delta_0^{\,3} + 0.4146\,\delta_0^{\,2} - 0.6867\,\delta_0 + 0.754 \quad (0.26 < \delta_0 < 5.08) \\ -1.182\times 10^{-4}\,\delta_0^{\,3} + 3.929\times 10^{-3}\,\delta_0^{\,2} \\ \qquad -5.017\times 10^{-2}\,\delta_0 + 0.3102 \qquad (5.08 < \delta_0 < 10.55) \\ 0.0452\left[(6.649+\delta_0)\log(1+6.649/\delta_0) - 6.649\right] (\delta_0 > 10.55), \end{cases} \tag{2.16}$$

where $t = \log(1/\delta_0) + 0.4513$ and f_{fit} is scaled with $3\pi\mu U a^2/\lambda_0$.

2.2. *Collisional dynamics*

We now turn our attention to finding the fractional energy loss in a particle collision. Davis (1984) has shown that van der Waals attractions can be important in promoting

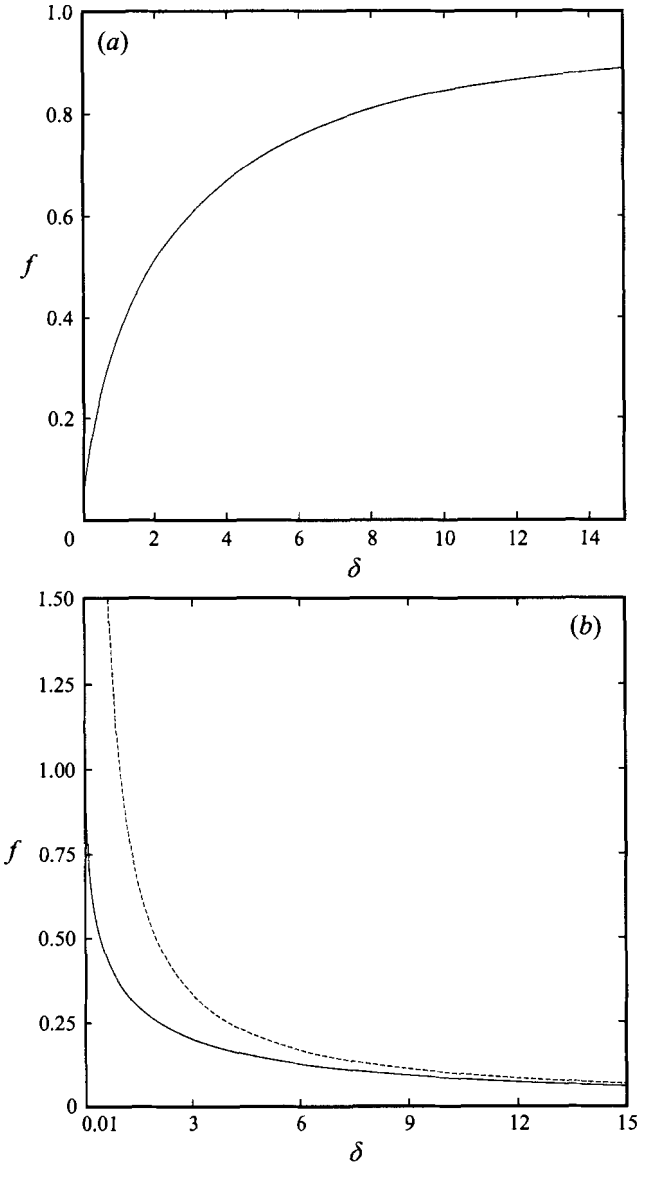

FIGURE 4. The force on the sphere as a function of the non-dimensional minimum gap thickness δ_0. (*a*) The force is scaled with the continuum lubrication resistance. (*b*) The force is scaled with $3\pi\mu Ua^2/\lambda_0$ so as to make the weaker divergence of the non-continuum force evident.

the gravity-induced coagulation in polydisperse aerosols with particle radii less than about 20 μm. In our analysis, we include only the lubrication resistance. However, the short-range van der Waals forces can be easily included in the analysis.

In describing particle collisions, it is customary to express the energy lost in the collision in terms of a coefficient of restitution e. The coefficient of restitution is defined as the ratio of the particles' relative velocity after collision to the velocity before collision. Let us consider the collision of two spheres with velocities $\pm U$. The

motion of the particles is governed by the equations

$$m\frac{\mathrm{d}U}{\mathrm{d}\tau} = -F$$

and

$$\frac{\mathrm{d}h}{\mathrm{d}\tau} = 2U\,,$$

with the initial conditions that at $\tau = 0$, $U = U_0$ and $h = h_0$. F is the lubrication resistance, U is the speed of the particle, m is the mass of the particle and the instant $\tau = 0$ corresponds to a gap thickness h_0 at which lubrication becomes effective. Jeffrey & Onishi (1984) have tabulated the resistance and mobility functions for two spheres in Stokes flow. From their calculations, one can identify the particle separation at which the force calculated using a series appropriate for small separations deviates from an asymptotic value appropriate for widely separated particles. This could then be taken to be the separation at which lubrication forces come into play. Though this choice depends on the criterion adopted to identify the deviation, it is not critical to the calculation of energy dissipation and we have chosen to introduce lubrication forces when the gap thickness is $0.1a$.

We now non-dimensionalize the velocity with the initial particle velocity U_0, the gap thickness h with h_0, and the time τ with h_0/U_0. Since the motion of the gas is quasi-steady, the force is proportional to the instantaneous velocity. In other words, the force F is given by

$$F = 3\pi\mu U_0 \frac{a^2}{h} u f\,,$$

where u is the dimensionless velocity and f is the dimensionless force given by (2.15). With these scalings and $\delta_0 = h_0/\lambda_0$, we obtain

$$\frac{\mathrm{d}u}{\mathrm{d}t} + \frac{\delta_0}{St}\frac{uf}{\delta} = 0\,, \quad \frac{\mathrm{d}\delta}{\mathrm{d}t} - 2\delta_0 u = 0\,, \tag{2.17}$$

where $St \equiv mU_0/3\pi\mu a^2$ is the Stokes number, which measures the relative importance of particle inertia and viscous dissipation, and t is the dimensionless time. The initial conditions are that at $t = 0$; $u = -1$ and $\delta = \delta_0$. The above equation has two parameters – St and δ_0. Now, the significant particle size range in cloud physics applications is 10–100 μm (Hocking 1973). Moreover, the mean-free path is approximately 0.1 μm. Thus, with $h_0 = 0.1a$, the values of δ_0 that are of practical interest range from 10 to 100.

Equation (2.17) can also be written as

$$\frac{\mathrm{d}u}{\mathrm{d}\delta} = \frac{-1}{2\,St}\frac{f}{\delta}\,. \tag{2.18}$$

The velocity of the particles can be determined as a function of gap thickness by integrating (2.18). For moderate or large Stokes numbers, the velocity will be non-zero when the particles come into contact. If we assume that the actual solid-body collision is perfectly elastic and continue the integration for the particle rebound using (2.18), we can determine the fraction of the particle energy that is lost during a collision and rebound in which the initial and final particle separations are $0.1a$. This fractional energy loss, $1 - e^2$, is

$$1 - e^2 = \frac{2}{St}\left(1 - \frac{1}{2St}(\log\delta_0 - 1.28)\right)(\log\delta_0 - 1.28)\,, \tag{2.19}$$

where e is the coefficient of restitution resulting from viscous forces. Equation (2.19) applies only when $St > (\log \delta_0 - 1.28)$. For smaller values of the Stokes number the particles' relative motion is arrested before their separation returns to $0.1a$. The fractional energy loss up to the point of impact, $1 - e_1^2$, is given by

$$1 - e_1^2 = \frac{1}{St}\left(1 - \frac{1}{4St}(\log \delta_0 - 1.28)\right)(\log \delta_0 - 1.28).$$

It may be noted that the leading behaviour of the fractional energy loss calculated by applying Hocking's result for the lubrication force to all particle separations is

$$1 - e^2 = \frac{2}{St}\left(1 - \frac{1}{2St}(\log \delta_0 - 1.28)\right)(\log \delta_0 - 0.12),$$

which is larger than that given by (2.19). This is due to the relatively strong divergence of the force given by Hocking's analysis.

3. Collision of cylinders

3.1. *Transitional flow*

In the previous section, we analysed the incompressible lubrication flow between two spheres in the limit $\lambda_0 \ll a\epsilon^{1/2}$. Our aim in this section is to study the incompressible, non-continuum lubrication flow between two cylinders. We first analyse the flow between two cylinders in the limit $a\epsilon \ll \lambda_0 \ll a\epsilon^{1/2}$ and then study the free molecular flow between cylinders.

Consider the normal motion of two equal-sized cylinders of radius a (figure 2). When $\lambda_0 \ll a\epsilon^{1/2}$, the collision of unequal-sized cylinders can be treated by defining $a = 2a_1a_2/(a_1 + a_2)$, where a_1 and a_2 are the radii of the cylinders. The speed of each cylinder is U and as before, $h_0 \equiv a\epsilon$ denotes the minimum gap thickness. The coordinate along the flow direction is x and that along the length of the cylinder is y. All distances in the x- and y-directions are scaled with $a\epsilon^{1/2}$ and those in the z-direction are scaled with $a\epsilon$. The number density of molecules in the bulk is given by n_0 and p_0 is the corresponding atmospheric pressure.

Since the geometry along the flow direction is the same for a sphere and a cylinder, we have the same asymptotic scalings for the pressure in both cases. The starting point, as before, is the integral mass balance equation. For cylinders, we have

$$\frac{\mathrm{d}}{\mathrm{d}x}\int_{-\bar{h}/2}^{+\bar{h}/2} u_x \,\mathrm{d}z = 2.$$

The rest of the analysis is similar to what we described for the case of spheres (see §2). The non-dimensional expression for the pressure is the same as (2.14), with the only difference that the pressure is now scaled with $6\mu Ua/h^2$, which is the continuum lubrication pressure for cylinders. It may be noted that, while the pressure is proportional to $1/h^2$ for both spheres and cylinders, the centreline pressure in the case of cylinders is twice that for spheres. Owing to cylindrical geometry, there is a net flow only in the x-direction. Thus, to drive the same mass flux, the pressure at the centreline is larger than that for spheres.

The lubrication force per unit length of cylinder can be found by integrating the pressure over the surface of the cylinder. Scaling the force with its continuum value

$3\pi\mu U a^{3/2}/2h^{3/2}$, we obtain the force to leading order to be

$$F = \frac{\pi^2 \mu U (a/\lambda_0)}{\epsilon^{1/2} \log(\lambda_0/a\epsilon)} \left[1 + O\left(\frac{1}{\log(\lambda_0/a\epsilon)}\right)\right]. \tag{3.1}$$

This is valid in the limit $a\epsilon \ll \lambda_0 \ll a\epsilon^{1/2}$. The non-continuum lubrication force has a much weaker divergence than the continuum force because the pseudo-Knudsen pressure scales like $\epsilon^{-1}/\log(\lambda_0/a\epsilon)$, as opposed to ϵ^{-2} in the continuum case.

3.2. *Free molecular flow*

In this section we consider the free molecular lubrication flow due to the normal relative motion of two cylinders. The velocity of the cylinders is $\pm U$. The ambient number density is n_0. The mean free path $\lambda_0 \gg a\epsilon^{1/2}$. We consider the case of small Mach numbers, i.e. $M \equiv U/\bar{c} \ll 1$.

When the mean free path is much larger than the distance $a\epsilon^{1/2}$ over which the effects of curvature become important, the flow in the gap can be treated as a free molecular flow. When the mean free path is of the same order as $a\epsilon^{1/2}$, the flux through a given cross-section depends on the number density of molecules at other points on the surface. This leads to an integral equation for the flux. As mentioned previously, the cases $\lambda_0 \gg a\epsilon^{1/2}$ and $\lambda_0 \sim O(a\epsilon^{1/2})$ do not contribute significantly to the energy dissipated in the collision. However, to illustrate the nature of this regime, we study the free molecular flow between two equal-sized cylinders. A calculation similar to the one detailed below may be performed for the case of colliding spheres, although the analysis would be much more complicated.

An equation for the number density can be obtained by observing that, at each point along the cylinder surface, the number of molecules coming in is equal to the number leaving. Another equivalent approach is to consider the net molecular flux out of the gap at any cross-section and equate it to the macroscopic flux set up by the relative motion of the spheres. As can be seen from figure 5, the molecular flux through any given cross-section is composed of two parts – one due to molecular exchange between the surfaces and the other due to molecules that escape to the bulk without colliding with a particle surface. We will refer to the latter as the 'direct contribution' to the flux through the gap at any given cross-section. We first consider this direct contribution and then combine it with the contribution to the flux coming from molecular exchange between surfaces. These in turn will be used to derive results for the pressure profiles and the force resisting motion.

3.2.1. *Direct contribution to molecular flux*

Before we proceed to calculate the contribution to the flux coming from molecules which escape directly to the bulk, we note that, for points on the cylinder such that $|x| > x_m > 0$, where $\pm x_m$ denote the points of common tangency of the cylinders, there is no flux to $-\mathrm{sgn}(x)\,\infty$ (see figure 5). Moreover, molecules emanating from any given point on the bottom surface can reach only the portion of the top surface that is not shielded from the point under consideration. For example, molecules leaving the bottom surface at x' in figure 5 can only fly to points between x'_- and x'_+ on the top surface.

In order to find the point of common tangency of the cylinders, we first write the equation of the tangent to the top cylinder (centred at $(0, 1 + \epsilon/2)$), from a point (x', z') on the bottom cylinder. The required equation is

$$x^2 - xx' + \epsilon\,(z^2 - zz') = (1 + \epsilon/2)\,(z - z'), \tag{3.2}$$

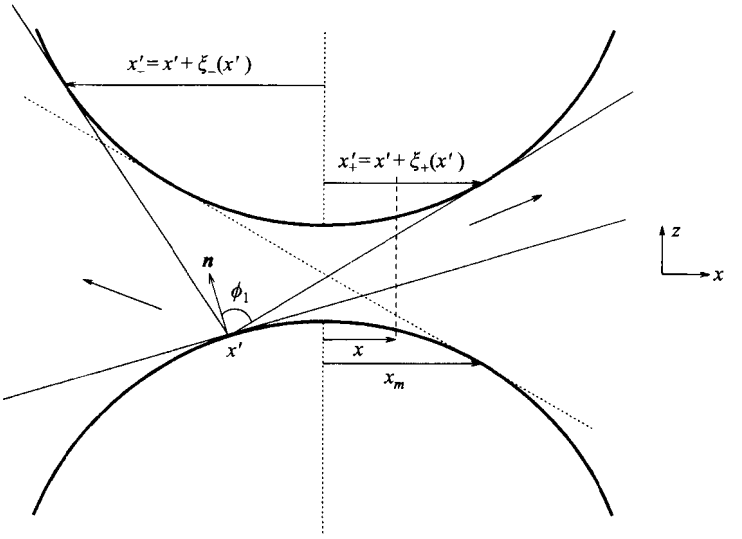

FIGURE 5. Schematic used in the analysis of the free molecular flow between two equal-sized cylinders. The angle between the normal to the bottom cylinder and the tangent to the top cylinder is denoted by ϕ_1. The abscissas of the points of common tangency are given by $\pm x_m$. There is a flux to both $+\infty$ and $-\infty$ only for $-x_m < x < +x_m$.

which represents a pair of straight lines. Retaining only the $O(1)$ terms in the above equation and using $|z| = (1+x^2)/2$, we obtain a quadratic equation for x, the solution of which is

$$x'_\pm = x' \pm [2(1+x'^2)]^{1/2} . \tag{3.3}$$

Here, $x'_\pm$ denote the x-coordinates of the points of tangency. From the above equation, it can be seen that the point of common tangency occurs at $\pm x_m$, where $x_m = 1$.

The net number of molecules leaving dx', per unit length of the cylinder, per unit time is given by

$$d\tilde{Q}_+ = (n(x') - n_0) a\epsilon^{1/2} dx' \int f(\boldsymbol{c})\boldsymbol{c}\cdot\boldsymbol{n} d\boldsymbol{c} .$$

Hence, the molecular flow rate to $+\infty$, per unit length of the cylinder, is given by

$$\tilde{Q}_+(x) = a\epsilon^{1/2} \int_{-1}^{x} (n(x') - n_0)\, dx' \int_{-\infty}^{\infty} dc_y \int_0^{\infty}\int_{\phi_1}^{\pi/2} f(c_\rho, c_y)\, c_\rho^2 \cos\phi\, dc_\rho\, d\phi . \tag{3.4}$$

Here, c is the molecular speed, ϕ is the angle between the normal to the bottom cylinder and the direction of flight of the molecule, and $f(c_\rho, c_y)$ is the usual Maxwellian velocity distribution written in appropriate cylindrical coordinates:

$$f(c_\rho, c_y) = \left(\frac{m}{2\pi kT}\right)^{3/2} \exp\left(\frac{-m(c_\rho^2 + c_y^2)}{2kT}\right).$$

On carrying out the integrals over c_ρ, c_y, and ϕ in (3.4), we obtain

$$Q_+(x) = \frac{1}{8}\int_{-1}^{x} v(x')\,(1 - \sin\phi_1(x'))\, dx' ,$$

where $\bar{c} = (8kT/\pi m)^{1/2}$, $v(x) \equiv (n(x) - n_0)/n_0$, and we have scaled the flow rate per unit length with $n_0 \bar{c}\, a\epsilon^{1/2}$.

From the definition of ϕ, it is clear that $\cos\phi_1 = \boldsymbol{n}_b \cdot \boldsymbol{e}_t$, where $\boldsymbol{n}_b$ is the unit normal to the bottom cylinder and $\boldsymbol{e}_t$ is the unit tangent to the top cylinder. We have

$$\boldsymbol{n}_b \approx \boldsymbol{e}_z + \epsilon^{1/2} x' \, \boldsymbol{e}_x + O(\epsilon),$$

and

$$\boldsymbol{e}_t \approx \boldsymbol{e}_x + \epsilon^{1/2} x'_+ \, \boldsymbol{e}_z + O(\epsilon),$$

where $\boldsymbol{e}_z$ and $\boldsymbol{e}_x$ are the unit vectors in the z- and x-directions respectively. This yields $\cos\phi_1 \approx \epsilon^{1/2}(x' + x'_+)$. Using this in the expression for the flow rate and accounting for both cylinders, the flow rate to $+\infty$ becomes

$$Q_+(x) = \frac{\epsilon}{8} \int_{-1}^{x} v(x') \, (x' + x'_+)^2 \, \mathrm{d}x'.$$

Similarly, the contribution to the molecular flow rate due to molecules going to $-\infty$ can be written as

$$Q_-(x) = -\frac{\epsilon}{8} \int_{x}^{+1} v(x') \, (x' + x'_-)^2 \, \mathrm{d}x',$$

where the negative sign in front of the integral indicates that the molecules going to $-\infty$ give a negative contribution to the overall flux.

Using these, the direct contribution Q_d to the overall flow rate Q through any cross-section can be written as

$$Q_d(x) = Q_+(x) \, H(x+1) + Q_-(x) \, H(1-x), \tag{3.5}$$

where $H(x)$ is the Heaviside step function and

$$Q_\pm(x) = \frac{\epsilon}{8} \int_{\mp 1}^{x} v(x') \, (x' + x'_\pm)^2 \, \mathrm{d}x', \tag{3.6}$$

with $x'_\pm = x' \pm [2(1 + x'^2)]^{1/2}$.

3.2.2. *Exchange contribution to the molecular flux*

In this section, we calculate the contribution to the overall flux through a given cross-section across the gap due to molecular exchange between the two surfaces. This contribution will henceforth be referred to as the 'exchange contribution'.

In discussing the direct contribution to the flux, we observed that, owing to the curvature of the particles, a cone of light emanating from a point on the bottom surface will illuminate only a portion of the top surface. This geometric constraint was used to determine the cutoff points for the direct contribution to the flux. We will similarly determine the cutoffs for the exchange contribution.

For any given x on the bottom cylinder, there is an exchange between the surfaces only for ξ such that the point $x + \xi$ on the top surface is visible from x. In other words, the exchange contribution is cut off when the line joining the points x and $x + \xi$ becomes tangential to either surface. Looking at figure 5, it becomes clear that, whenever $x < x_m$ (for any ξ) or $x > x_m$ ($\xi > 0$), this cutoff occurs when the line drawn from x is tangential to the top surface at $x + \xi_\pm$. Substituting $x + \xi_\pm$ for $x_\pm$ in (3.3), we obtain $\xi_\pm = \pm[2(1 + x^2)]^{1/2}$, where the positive and negative signs apply for $\xi > 0$ and $\xi < 0$ respectively. When $x > x_m$ ($\xi < 0$), the tangent to the bottom surface separates the top surface into regions visible and invisible as seen from x. Thus, setting $x_+ = x$ and $x' = (x + \xi_c)$ in (3.3), we obtain

$$\xi_c^2 + 4x\xi_c + 2(1 + x^2) = 0.$$

This can be solved to yield $\xi_c = -2x + [2(x^2-1)]^{1/2}$, where we have retained only the physically meaningful root.

The net number of molecules emitted per unit time, from a point $(x', y', z(x'))$ on the bottom cylinder and reaching the top surface at $(x'', y'', z(x''))$, is given by

$$\mathrm{d}\tilde{Q}_e = a\epsilon\,\mathrm{d}x'\,(n(x') - n(x''))\int_0^\infty \boldsymbol{c}\cdot\boldsymbol{n}_b\, f(\boldsymbol{c})\, c^2 \mathrm{d}\boldsymbol{c}\ ,$$

where $\mathbf{n}_b$ is the normal to the bottom surface. Introducing $\boldsymbol{e}_r \equiv \boldsymbol{c}/c$, integrating over c, and scaling $\tilde{Q}_e$ with $n_0\bar{c}\,a\epsilon^{1/2}$, this can be written as

$$\mathrm{d}Q_e = \mathrm{d}x'\,(v(x') - v(x''))\,|\Omega\cdot\boldsymbol{n}_b(x')|\mathrm{d}\Omega\ ,$$

where $v(x) = (n(x) - n_0)/n_0$ as before, and $\mathrm{d}\Omega$ is the solid angle subtended by the area element at the point of interest. Using $\boldsymbol{e}_r = \boldsymbol{r}/|\boldsymbol{r}|$, and $\mathrm{d}\Omega = \mathrm{d}x''\mathrm{d}y''|\mathbf{n}_t(x'')\cdot\boldsymbol{r}|/r^3$, where $\boldsymbol{r} = \mathbf{x}'' - \mathbf{x}'$, the flow rate of molecules crossing the cross-section from left to right at x per unit length in the y-direction can be written as

$$Q_{e+} = \frac{1}{4\pi}\int_{-\infty}^{\infty}\mathrm{d}y''\int_{x+\xi_{min}(x)}^{x}\mathrm{d}x'\int_{x}^{x'+\xi_{max}(x')}\mathrm{d}x''\,(v(x') - v(x''))\,\frac{|\boldsymbol{n}_b(x')\cdot\boldsymbol{r}|\,|\boldsymbol{n}_t(x'')\cdot\boldsymbol{r}|}{r^4}.$$

The cutoff limits ξ_{max} and ξ_{min} are given by: $\xi_{max} = [2(1+x^2)]^{1/2}$, $\xi_{min} = -2x + [2(x^2-1)]^{1/2}$ for $x > x_m$ and $\xi_{min} = -[2(1+x^2)]^{1/2}$ for $x \leqslant x_m$.

In addition to the molecules crossing the cross-section from left to right, giving a positive contribution to the net flux in the positive x-direction, there are molecules which travel from right to left, thereby giving a negative contribution to the flux. This contribution can be written as

$$Q_{e-} = -\frac{1}{4\pi}\int_{-\infty}^{\infty}\mathrm{d}y''\int_{x}^{x+\xi_{max}(x)}\mathrm{d}x'\int_{x'+\xi_{min}(x')}^{x}\mathrm{d}x''\,(v(x') - v(x''))\,\frac{|\boldsymbol{n}_b(x')\cdot\boldsymbol{r}|\,|\boldsymbol{n}_t(x'')\cdot\boldsymbol{r}|}{r^4},$$

where the negative sign in front indicates that Q_{e-} provides a negative contribution to the overall flux. The net flow rate in the positive x-direction, per unit length of cylinder, is given by

$$Q_e = Q_{e+} + Q_{e-}\ ,$$

where Q_{e+} and Q_{e-} are as discussed above.

For future use, it is convenient to differentiate this expression with respect to x. The result is

$$\frac{\mathrm{d}Q_e}{\mathrm{d}x} = A_1 + A_2, \tag{3.7}$$

where

$$A_1 = -\frac{1}{4\pi}\int_{-\infty}^{\infty}\mathrm{d}y''\int_{x+\xi_{min}(x)}^{x+\xi_{max}(x)}\mathrm{d}x''\,(v(x'') - v(x))\,\frac{|\boldsymbol{n}_b(x)\cdot\boldsymbol{r}|\,|\boldsymbol{n}_t(x'')\cdot\boldsymbol{r}|}{r^4},$$

$$A_2 = -\frac{1}{4\pi}\int_{-\infty}^{\infty}\mathrm{d}y''\int_{x+\xi_{min}(x)}^{x+\xi_{max}(x)}\mathrm{d}x'\,(v(x') - v(x))\,\frac{|\boldsymbol{n}_b(x')\cdot\boldsymbol{r}|\,|\boldsymbol{n}_t(x)\cdot\boldsymbol{r}|}{r^4},$$

and $r^2 = (x-x'')^2 + y''^2 + \epsilon(z(x) - z(x''))^2$. For convenience, we define $\xi \equiv x'' - x$, $h \equiv z(x'') - z(x)$. Using $|z(x)| = \frac{1}{2}(1+x^2)$, we can write $h = 1 + \frac{1}{2}(x^2 + (x+\xi)^2)$. Using these, and carrying out the integral involving y, we obtain

$$\frac{\mathrm{d}Q_e}{\mathrm{d}x} = -\frac{\epsilon}{4}\int_{\xi_{min}}^{\xi_{max}}\mathrm{d}\xi\,\frac{[v(x+\xi) - v(x)]\;G(x,\xi)}{\left[\xi^2 + \epsilon h^2\right]^{3/2}}, \tag{3.8}$$

where $G(x,\xi) = |h + x\xi||\xi(x+\xi) - h|$. It may be noted that, owing to symmetry, only positive values of x need be considered.

The total flow rate $Q(x) = Q_d(x) + Q_e(x)$, where Q_d and Q_e are as discussed above. We can write

$$\frac{dQ}{dx} = \frac{dQ_d}{dx} + \frac{dQ_e}{dx}, \tag{3.9}$$

where

$$\frac{dQ_d}{dx} = \frac{\epsilon}{8} v(x) \left[H(x+1)(x+x_+)^2 + H(1-x)(x+x_-)^2\right], \tag{3.10}$$

and

$$\frac{dQ_e}{dx} = -\frac{\epsilon}{4} \int_{\xi_{min}}^{\xi_{max}} d\xi \frac{[v(x+\xi) - v(x)]\ G(x,\xi)}{\left[\xi^2 + \epsilon(1+x^2)^2\right]^{3/2}}, \tag{3.11}$$

where we have approximated h as $1 + x^2$. This is valid because the term $\epsilon(1+x^2)^2$ in the integrand above becomes important only when $\xi \ll 1$.

We now define

$$v(x+\xi) \equiv v(x) + \xi \frac{dv}{dx} + \frac{\xi^2}{2} \frac{d^2v}{dx^2} + R(x,\xi).$$

Using this in the expression for dQ_e/dx and carrying out the integrals, we obtain

$$\frac{dQ_e}{dx} = -\frac{\epsilon}{4}(A + B + C + D),$$

where

$$A = J_1(x) \log \frac{1}{\epsilon},$$

$$B = J_1(x) \left(-2 + \log \frac{4|\xi_{max}\, \xi_{min}|}{(1+x^2)^2}\right),$$

$$C = \int_{\xi_{min}}^{\xi_{max}} d\xi \frac{J_2(x,\xi)}{|\xi|^3},$$

with

$$J_1(x) = 2x(1+x^2)\frac{dv}{dx} + \tfrac{1}{2}(1+x^2)^2 \frac{d^2v}{dx^2},$$

$$J_2(x,\xi) \equiv O + E,$$

$$O \equiv (1+x^2)^2 \frac{dv}{dx}\xi + x(1+x^2)\frac{d^2v}{dx^2}\xi^3 + \left(-\frac{1}{4}\frac{dv}{dx} - \frac{1}{2}x\frac{d^2v}{dx^2}\right)\xi^5,$$

$$E \equiv -x\frac{dv}{dx}\xi^4 - \frac{1}{8}\frac{d^2v}{dx^2}\xi^6,$$

and

$$D \equiv \int_{\xi_{min}}^{\xi_{max}} d\xi \frac{R(x,\xi)\, G(x,\xi)}{|\xi|^3}.$$

Note that the term A represents the singular part of the number density. It can also be observed that the leading behaviour of the number density is $O(1/\epsilon \log(1/\epsilon))$. This results in a force that scales like $(a/\lambda_0)\epsilon^{-1/2}/\log(1/\epsilon)$. In the pseudo-Knudsen limit, $\lambda_0 \ll a\epsilon^{1/2}$, the force scales like $(a/\lambda_0)\epsilon^{-1/2}/\log(\lambda_0/a\epsilon)$, while the continuum lubrication resistance scales like $1/\epsilon^{3/2}$.

3.3. *Pressure and force profiles*

In order to solve for the number density (and hence, the pressure), we equate the free molecular flow rate derived above to the flow rate obtained by an integral mass balance across the gap. The flow rate is given by

$$\tilde{Q}(x) = n_0 \int_{-h/2}^{h/2} \tilde{u}_x(z) \mathrm{d}\tilde{z}\,.$$

From the mass conservation equation we obtain

$$\frac{\mathrm{d}\tilde{Q}}{\mathrm{d}\tilde{x}} = 2n_0 U\,,$$

where U is the velocity of each cylinder. Combining this with (3.9), we obtain

$$\tfrac{1}{2}\nu(x)\left[H(x+1)(x+x_+)^2 + H(1-x)(x+x_-)^2\right] - (A+B+C+D) = 1\,, \qquad (3.12)$$

where we have now rescaled $\nu(x)$ with $8U/\bar{c}\epsilon$. The above equation is solved using a finite difference scheme. The boundary conditions are that the number density approaches the bulk number density far from the particles and that $n(x)$ is symmetric about $x = 0$. Using the pressure profiles so obtained, we can perform a numerical integration over the cylinder surface to obtain the force resisting relative motion. The result of this calculation is plotted in figure 6. For 1–100μm radius particles colliding in air ($\lambda_0 = 0.1\mu$m), the values of ϵ for which we have a free molecular flow range from 10^{-4}–10^{-8}. Here we have scaled the force with $2\pi^2\mu U(a/\lambda_0)\epsilon^{-1/2}/\log(1/\epsilon)$, which is the asymptotic behaviour of the force as the particle separation goes to zero. The correction to this leading behaviour is smaller by an $O(1/\log(1/\epsilon))$ factor. It is interesting to note the similarity of this leading behaviour with that in the limit $a\epsilon \ll \lambda_0 \ll a\epsilon^{1/2}$. In both cases, there is a factor of the form $\epsilon^{-1/2}/\log(r_c/a\epsilon)$, where r_c is a cutoff distance for the molecular flux. In the pseudo-Knudsen regime, this cutoff is the mean free path λ_0. In the free molecular flow case, the molecules travel a distance $O(a\epsilon^{1/2})$ before undergoing any collisions, making $a\epsilon^{1/2}$ the cutoff length. This suggests that the force scaling for free molecular flow between spheres is similar to that given by our pseudo-Knudsen regime analysis, except that λ_0 is now replaced by $a\epsilon^{1/2}$. Thus, we conclude that, for spheres, the free molecular lubrication force diverges like $\log\log(1/\epsilon)$.

4. Conclusions

In this paper, we have studied the incompressible lubrication flows between two spheres. We have also analysed the nature of the lubrication resistance for the case of two cylinders. By making certain approximations which are valid when we have a lubrication flow and when the Mach number is small, we have been able to analyse the leading behaviour of the lubrication resistance for all particle separations.

When $a\epsilon \ll \lambda_0 \ll a\epsilon^{1/2}$, we have shown that the force resisting the normal motion of two spheres has a rather weak $\log\log(\lambda_0/a\epsilon)$ divergence with decreasing particle separation. In deriving this result, we used an asymptotic expression for the pseudo-Knudsen flux derived in the Appendix. This pseudo-Knudsen flux has a logarithmically large contribution from molecules that travel large distances ($\sim \lambda_0$) nearly parallel to the channel walls. We have derived the leading logarithmic behaviour as well as the $O(1)$ correction to it. Prior to our analysis, there have been many studies which have obtained the leading logarithmic behaviour. Our calculation provides

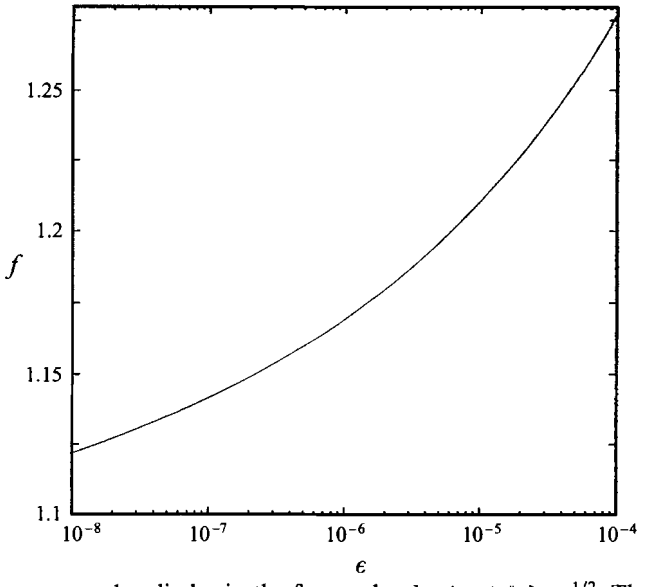

FIGURE 6. The force on each cylinder in the free molecular limit $\lambda_0 \gg a\epsilon^{1/2}$. The force is scaled with the leading behaviour in the free molecular case, so that as ϵ goes to zero, the force approaches unity.

an analytical expression for the flux valid in the high Knudsen number limit. The available approximations are in good agreement with our exact result.

We have also shown that, for large particle inertia, the fraction of the total energy dissipated by viscous forces during a collision between two spheres is $(2/St)(\log \lambda_0/h_0 - 1.28)$, where $St = mU_0/3\pi\mu a^2$ is the Stokes number. This allows us to deduce the critical Stokes number below which the particles lose all their kinetic energy before bouncing back to their initial separation. The criterion for such a sticking is $St > (\log(\lambda_0/h_0) - 1.28)$.

The mobility of two spherical particles moving towards each other is often required in theoretical and numerical studies of a suspension of hydrodynamically interacting spherical particles. However, results for the mobility were not available previously over the entire range of particle separations. Ying & Peters (1989) have provided results for $\lambda_0 \gg a\epsilon$, with $\epsilon \sim O(1)$. These results together with ours for $\epsilon \ll 1$ with $a\epsilon/\lambda_0 \sim O(1)$ enable the calculation of mobility for all separations.

In § 3, we analysed the flow between two cylinders. When $\lambda_0 \ll a\epsilon^{1/2}$, the flow field is locally the same for sphere–sphere and cylinder–cylinder collisions. Hence the scalings for the flux and the pressure profiles are the same in both cases. For cylinders, with separations such that $a\epsilon \ll \lambda_0 \ll a\epsilon^{1/2}$, the lubrication force scales like $\pi^2\mu U_0 a^{3/2}/(\lambda_0 h_0^{1/2} \log(\lambda_0/h_0))$, which is weaker than the $h_0^{-3/2}$ divergence seen in the continuum case.

We have also analysed the free molecular flow between cylinders, corresponding to $\lambda_0 \gg a\epsilon^{1/2}$, and obtained results for the force. When $\lambda_0 \gg a\epsilon^{1/2}$, the nature of the flow in the gap is vastly different from that for $a\epsilon \ll \lambda_0 \ll a\epsilon^{1/2}$. In this free molecular flow case, the relationship between the flux and the pressure gradient is no longer local. The leading behaviour of the force in this case is $2\pi^2\mu U(a/\lambda_0)\epsilon^{-1/2}/\log(1/\epsilon)$ and the pressure scales with $\epsilon^{-1}/\log(1/\epsilon)$. The asymptotic scalings for the force corresponding to the pseudo-Knudsen and free molecular regimes can be cast in the form $\pi^2\mu U(a/\lambda_0)\epsilon^{-1/2}/\log(r_c/a\epsilon)$, where r_c is a cutoff distance for the molecular

flux. In the pseudo-Knudsen regime, the flux is cut off by the mean free path ($r_c = \lambda_0, a\epsilon \ll \lambda_0 \ll a\epsilon^{1/2}$). When $\lambda_0 \gg a\epsilon^{1/2}$, the flux is cut off by the curvature of the particles, leading to $r_c = a\epsilon^{1/2}$. These observations allow us to deduce that, for the collision of spheres, the free molecular lubrication force diverges like (cf. equation (2.15)) $\pi^2 \mu U (a^2/2\lambda_0) \log\log(1/\epsilon)$.

This work was supported by the US Environmental Protection Agency under grant number R81-9761-010. Preliminary work on this problem was conducted in collaboration with Srinivasan Rengaswamy, a Masters student under D. L. K.'s supervision.

Appendix. Molecular flux in Poiseuille channel flow

The pressure-driven flow of a rarefied gas in a channel has been studied extensively (Hickey & Loyalka 1984; Cercignani & Daneri 1961, to cite a few examples). These studies have concentrated primarily on the cases $h \sim \lambda_0$ and $h \gg \lambda_0$, where h is the channel width and λ_0 is the mean free path. While these studies have also established the leading behaviour of the flux in the limit $h \ll \lambda_0$, a direct, analytical derivation – based on simple physical reasoning – has been lacking so far. In this Appendix, we derive the leading logarithmic behaviour of the flux, and the $O(1)$ correction to it.

For very small gap thicknesses $h_0 \ll \lambda_0$, one might expect the flow in the gap to be governed by a Knudsen diffusion of the gas molecules between the particles (approximated locally as two flat plates). However, an attempt to calculate the Knudsen diffusivity for pressure-driven flow between two flat plates leads to a logarithmically divergent integral. This divergence is due to a large contribution to the flux through a given cross-section, coming from molecules that travel a large distance nearly parallel to the channel surface. If the molecule travels a distance comparable to the mean free path, it will undergo an intermolecular collision. This collision is likely to yield a velocity that is not nearly parallel to the walls and hence the molecule will be driven to the wall in an $O(h_0)$ distance. The result is a flux that is similar to that given by Knudsen diffusion, but with a 'pseudo-Knudsen diffusivity' that is proportional to $\bar{c}\, h_0 \log(\lambda_0/h_0)$ instead of $\bar{c}\, h_0$, where $\bar{c} = (8kT/\pi m)^{1/2}$ is the mean molecular speed. (Here k is the Boltzmann constant, T is the temperature of the gas and m is the molecular mass.)

A.1. *Flux versus pressure gradient relation for* $a\epsilon \ll \lambda_0 \ll a\epsilon^{1/2}$

Consider the isothermal, pressure-driven flow of a gas in a channel made of two parallel plates of infinite extent separated by a distance h, as shown in figure 7. The gas molecules are hard spheres of mass m and the temperature is T. In order to derive the 'pseudo-Knudsen flux', the gas is assumed to be only slightly perturbed from its equilibrium Maxwell distribution $f(\mathbf{c})$. This will be true for small values of the pressure gradient such that, in the region of interest,

$$\frac{|\mathrm{d}n/\mathrm{d}x|}{|\mathrm{d}^2 n/\mathrm{d}x^2|} \gg \lambda_0 .$$

The gas flow is in the x-direction. The number density, $n(x)$, may be approximated locally as a linear function of x:

$$n(x) = n_0 + \frac{\mathrm{d}n}{\mathrm{d}x}\, x . \tag{A 1}$$

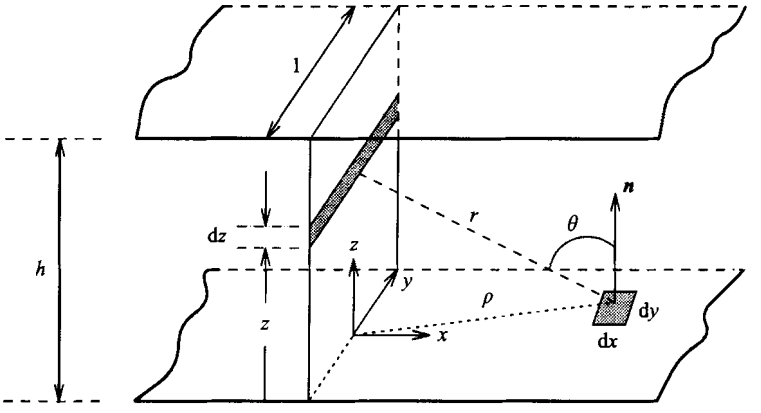

FIGURE 7. Schematic used in the derivation of the pseudo-Knudsen flux due to a pressure-driven flow in a channel. The two flat plates are separated by a distance h in the z-direction and are infinite in extent in the other two directions. The unit-normal to the plate is $\boldsymbol{n}$.

The molecular flux is defined to be the number of molecules passing through a unit cross-section of the channel in unit time. There are two contributions to this flux. One is due to molecules emitted from the wall and passing through the cross-section without undergoing any intermolecular collisions. The other contribution to the flux comes from molecules which pass through the cross-section after undergoing an intermolecular collision.

The flux due to molecules emitted from the surface is calculated as follows. Assuming that the molecules are diffusely emitted from the wall, the number of molecules coming from an area $(\mathrm{d}x\,\mathrm{d}y)$ and passing through an element of the cross-section in unit time is

$$\mathrm{d}Q_w = (\mathrm{d}x\,\mathrm{d}y)\; n(x) \int_{c=0}^{\infty} c_z\; f(c)\; c^2\; \mathrm{d}c\; \mathrm{d}\Omega\;.$$

Here, $r^2 = (x^2 + y^2 + z^2)$, $\mathrm{d}\Omega = -x\,\mathrm{d}z/r^3$ is the solid angle subtended by the cross-section element at the point of interest on the wall, and $f(c) = (m/2\pi kT)^{3/2}$ $\exp(-mc^2/2kT)$ is the Maxwellian velocity distribution function. Of the molecules moving at speed c, only a fraction, $\mathrm{e}^{-r/\lambda(c)}$, travel at least a distance r (see chapter 5 of Chapman & Cowling 1990). $\lambda(c)$ is the speed-dependent mean free path, which is given by

$$\lambda(c) = \frac{\lambda_0}{\psi(s)}\,, \tag{A 2}$$

where λ_0 is the mean free path of the hard-sphere gas, $s = c\,\left(m/2kT\right)^{1/2}$, and

$$\psi(s) = \frac{1}{s^2(2\pi)^{1/2}}\left(s\,\mathrm{e}^{-s^2} + (2s^2+1)\int_0^s \mathrm{e}^{-\eta^2}\mathrm{d}\eta\right). \tag{A 3}$$

Taking account of this survival probability and also the contribution from both walls, the total flow rate becomes

$$Q_w = 2\iiint \mathrm{d}x\,\mathrm{d}y\; n(x)\,\mathrm{e}^{-r/\lambda(c)}\; c^3\; f(c)\; \mathrm{d}c\; \cos(\theta)\; \mathrm{d}\Omega\,.$$

Using $\mathrm{d}\Omega = -x\,\mathrm{d}z/r^3$, $\cos(\theta) = z/r$, $n(x) = n_0 + x\,\mathrm{d}n/\mathrm{d}x$, and rearranging, we obtain

$$Q_w = -2\frac{\mathrm{d}n}{\mathrm{d}x}\int_0^\infty c^3 f(c)\,\mathrm{d}c \int_{-\infty}^{\infty}\int_{-\infty}^{\infty} x^2\,\mathrm{d}x\,\mathrm{d}y \int_0^h \mathrm{e}^{-r/\lambda(c)}\,\frac{z\,\mathrm{d}z}{r^4}\,. \tag{A 4}$$

Using cylindrical-polar coordinates $x = \rho\cos\phi$, $y = \rho\sin\phi$ and $r^2 = \rho^2 + z^2$ and evaluating the resulting iterated integral, we obtain

$$Q_w = -2\pi\frac{\mathrm{d}n}{\mathrm{d}x}\int_0^\infty c^3 f(c)\,\mathrm{d}c\, I(c).$$

Here, $I(c)$ is given by

$$I(c) = I_1(c) + I_2(c), \tag{A 5}$$

where

$$I_1(c) = \frac{\lambda^2(c)}{4}\left(1 - \mathrm{e}^{-h/\lambda(c)} - \frac{h}{\lambda(c)}\,\mathrm{e}^{-h/\lambda(c)}\right),$$

and

$$I_2(c) = \frac{h^2}{2}\int_h^\infty \mathrm{e}^{-r/\lambda(c)}\,\frac{\mathrm{d}r}{r} - \frac{h^4}{4}\int_h^\infty \mathrm{e}^{-r/\lambda(c)}\,\frac{\mathrm{d}r}{r^3}\,.$$

Now, using (A 2) for $\lambda(c)$, we can write the flow rate as

$$Q_w = -h^2\,\bar{c}\,\frac{\mathrm{d}n}{\mathrm{d}x}\int_0^\infty G(\delta\,\psi(s))\,s^3\,\mathrm{e}^{-s^2}\,\mathrm{d}s, \tag{A 6}$$

where

$$G(\delta\psi) = \frac{1}{4(\delta\psi)^2}\left(1 - \mathrm{e}^{-\delta\psi} - \delta\psi\,\mathrm{e}^{-\delta\psi}\right) + \tfrac{1}{2}\left(E_1(\delta\psi) - \tfrac{1}{2}E_3(\delta\psi)\right). \tag{A 7}$$

The functions $E_1(s)$ and $E_3(s)$ are the exponential integrals defined by (see chapter 5 of Abramowitz & Stegun 1993)

$$E_n(s) = \int_1^\infty \frac{\mathrm{e}^{-st}}{t^n}\mathrm{d}t, \quad n = 1, 2, 3\ldots\,.$$

We are interested in evaluating Q_w in the asymptotic limit $\delta \to 0$. For this we note that the asymptotic behaviour of $\lambda(c)$ is different in the two limits $c \to 0$ and $c \to \infty$. This can be seen by examining the function $\psi(s)$, which has the following asymptotic forms:

$$\left.\begin{aligned} \psi(s) &\sim \left(\frac{2}{\pi}\right)^{1/2}\frac{1}{s} && \text{as } s \to 0, \\ \psi(s) &\sim \frac{1}{\sqrt{2}}\left(1 + \frac{1}{2s^2}\right) && \text{as } s \to \infty. \end{aligned}\right\} \tag{A 8}$$

From this it can be seen that the behaviour of the integrand in (A 6) is different in the two regions $s \ll \delta \ll 1$ (the *inner* region) and $\delta \ll s$ ($\delta \to 0$) (the *outer* region). Using the method of matched asymptotic expansions, it can be shown that the contribution to the flux from the inner region, corresponding to $c \ll 1$ ($h \to 0$), is negligible compared to that from the outer region.

It can be shown that for $\delta \ll 1$, the asymptotic behaviour of the flux $q_w \equiv Q_w/h$, is

$$q_w = -\frac{\mathrm{d}n}{\mathrm{d}x}\frac{h\bar{c}}{4}\left(-\log(\delta) - \gamma - 2\int_0^\infty s^3 \mathrm{e}^{-s^2}\log(\psi(s))\,\mathrm{d}s + O(\delta)\right), \tag{A 9}$$

where $\gamma \approx 0.57721\ldots$ is Euler's constant.

We now proceed to calculate the contribution to the flux due to molecules passing through the cross-section after undergoing an intermolecular collision more recently than a collision with one of the walls. The rate of intermolecular collisions (for molecules of speed c) is $c/\lambda(c)$. The number of molecules coming from an element $(\mathrm{d}x'\,\mathrm{d}y'\,\mathrm{d}z')$ and passing through the cross-section is

$$\mathrm{d}Q_c = \int_{c=0}^{\infty} \mathrm{e}^{-r/\lambda(c)}\frac{c}{\lambda(c)}\,c^2 f(c)\,\mathrm{d}c\; n(x')\,\mathrm{d}x'\,\mathrm{d}y'\,\mathrm{d}z'\;\mathrm{d}\Omega\,.$$

Here, $\mathrm{d}\Omega = -x'\,\mathrm{d}z/r^3$ is the solid-angle element mentioned previously. The total flow rate is

$$Q_c = -\pi\frac{\mathrm{d}n}{\mathrm{d}x}\int_{-\infty}^{\infty}\int_{-\infty}^{\infty} x'^2\,\mathrm{d}x'\,\mathrm{d}y'\int_0^h \mathrm{d}z'\int_0^h \frac{\mathrm{d}z}{r^3}\int_0^\infty \mathrm{e}^{-r/\lambda(c)}\frac{c^3}{\lambda(c)}f(c)\,\mathrm{d}c\,. \tag{A 10}$$

This integral can be evaluated by a procedure similar to that used in the evaluation of Q_w. The asymptotic behaviour of the flux $q_c \equiv Q_c/h$ in the limit $\delta \ll 1$ can then be shown to be

$$q_c = -\frac{\mathrm{d}n}{\mathrm{d}x}\left(\frac{h\,\bar{c}}{4}\right) + O(\delta)\,. \tag{A 11}$$

The overall flux $q = q_w + q_c$ becomes

$$q = -\frac{\mathrm{d}n}{\mathrm{d}x}\frac{h\bar{c}}{4}\left(-\log(\delta) + 1.0 - \gamma - 2\int_0^\infty s^3\mathrm{e}^{-s^2}\log\psi(s)\,\mathrm{d}x + O(\delta)\right).$$

Evaluating the integral involving $\psi(s)$ numerically, we obtain

$$q = -\frac{\mathrm{d}n}{\mathrm{d}x}\frac{h\,\bar{c}}{4}\,(-\log(\delta) + 0.4513 + O(\delta))\,. \tag{A 12}$$

This expression gives the leading behaviour of the pseudo-Knudsen flux and the order-one correction to it. It may be noted that this expression is exact in the asymptotic limit $\delta \ll 1$.

The nearly incompressible pressure-driven flow of a rarefied gas in a channel, which, for small Mach numbers, is governed by the linearized Boltzmann equation, has been the subject of many articles in the literature. Hickey & Loyalka (1990) have solved the linearized Boltzmann equation in its exact form. (However, their numerical results are not available over a wide range of Knudsen numbers.) On the other hand, solutions of approximate forms of the governing equation are also available. For example, Cercignani (1963) uses the BGK model for the collision operator and obtains an asymptotic expression for the flux valid in the limit $\delta \ll 1$. It is of interest to compare the flux given by (A 12) with the asymptotic form of the flux obtained by solving a linearized form of the Boltzmann equation. We compare our pseudo-Knudsen flux expression with the flux obtained by Cercignani.

Cercignani (1963) starts his analysis with the BGK approximation to the linearized Boltzmann equation and reduces the problem of finding the flux to one of solving an integral equation (for details, see Cercignani 1963). The integral equation is solved by an iteration procedure. By stopping at the first step in the iteration, Cercignani was

able to recover the leading $\log(1/\delta)$ behaviour for the flux. We have computed the $O(1)$ correction to this and the result is

$$q = -\frac{\mathrm{d}n}{\mathrm{d}x}\frac{h\bar{c}}{4}(-\log\delta + 0.4786). \tag{A 13}$$

As can be seen, the expression obtained using the BGK model agrees well with our exact result (A 12). The $O(1)$ term in the expression above was obtained by evaluating the quantity Q_1, defined by equation (27) in Cercignani (1963). It can be shown that further iterations do not contribute to the $O(1)$ term and hence it is sufficient to evaluate Q_1 alone in order to obtain the order-one correction. In obtaining (A 13), we have converted the mean free path λ_B used by Cercignani to the mean free path λ_0 of a hard-sphere gas by using the relation $\lambda_B = \pi^{1/2}\lambda_0$ (Cercignani 1975).

REFERENCES

Abramowitz, M. & Stegun, I. A. 1993 *Handbook of Mathematical Functions.* Dover.

Barnocky, G. & Davis, R. H. 1989 The influence of pressure dependent density and viscosity on the elastohydrodynamic collision and rebound of two spheres. *J. Fluid Mech.* **209**, 501.

Bender, C. L. & Orszag, S. A. 1978 *Advanced Mathematical Methods for Scientists and Engineers.* McGraw-Hill.

Bohnet, M. 1983 In *Handbook of Fluids in Motion* (ed. N. P. Cheremisinoff & R. Gupta). Ann Arbor.

Cercignani, C. 1963 Plane poiseuille flow and Knudsen minimum effect. In *Rarefied gas dynamics* (ed. J. A. Laurmann), vol. 2, p. 92. Academic.

Cercignani, C. 1975 *Theory and Application of the Boltzmann Equation.* Elsevier.

Cercignani, C. & Daneri, A. 1963 Flow of a rarefied gas between two parallel plates. *J. Appl. Phys.* **34**, 3509.

Chapman, S. & Cowling, T. G. 1990 *The Mathematical Theory of Non-uniform Gases.* Cambridge University Press.

Davis, R. H. 1984 The rate of coagulation of a dilute polydisperse system of sedimenting spheres. *J. Fluid Mech.* **145**, 179.

Davis, R. H., Serraysol, J. & Hinch, E. J. 1986 The elastohydrodynamic collisions of two spheres. *J. Fluid Mech.* **163**, 479.

Hickey, K. A. & Loyalka, S. K. 1990 Plane poiseuille flow: Rigid sphere gas. *J. Vac. Sci. Technol.* A **8**, 957.

Hocking, L. M. 1973 The effect of slip on the motion of a sphere close to a wall and of two adjacent spheres. *J. Engng Maths* **7**, 207.

Hocking, L. M. & Jonas, P. R. 1970 The collision efficiency of small drops. *Q. J. R. Met. Soc.* **96**, 722.

Jeffrey, D. J. & Onishi, Y. 1984 Calculation of the resistance and mobility functions for two unequal sized spheres in low-Reynolds-number flow. *J. Fluid Mech.* **139**, 261.

Jenkins, J. T. & Savage, S. B. 1983 A theory for the rapid flow of identical, smooth, nearly elastic spherical particles. *J. Fluid Mech.* **130**, 187.

Koch, D. L. 1990 Kinetic theory for a monodisperse gas-solid suspension. *Phys. Fluids* A **2**, 1711.

Kumaran, V. & Koch, D. L. 1993 Properties of a bidisperse particle-gas suspension. Part 1. Collision time small compared with viscous relaxation time. *J. Fluid Mech.* **247**, 623.

Kytömaa, H. K. & Schmid, P. J. 1992 On the collision of rigid spheres in a weakly compressible fluid. *Phys. Fluids* A **4**, 2683.

Loyalka, S. K. & Ferziger, J. H. 1967 Model dependence of the slip coefficient. *Phys. Fluids* **10**, 1833.

Ochs, H. T. & Beard, K. V. 1985 Effects of coalescence efficiencies on the formation of precipitation. *J. Atmos. Sci.* **42**, 1451.

Ying, R. & Peters, M. H. 1989 Hydrodynamic interaction of two unequal-sized spheres in a slightly rarefied gas: resistance and mobility functions. *J. Fluid Mech.* **207**, 353.